Eur. Phys. J. B **41**, 55–60 (2004)
DOI: 10.1140/epjb/e2004-00293-7

THE EUROPEAN PHYSICAL JOURNAL B

Static magnetic susceptibility of the RbC_{60} polymerized fulleride

V. Likodimos[1], S. Glenis[2,a], and C.L. Lin[3]

[1] Physics Department, National Technical University, 157 80 Athens, Greece
[2] Department of Physics, University of Athens, 157 84 Athens, Greece
[3] Department of Physics, Temple University, Philadelphia, PA 19122, USA

Received 4 June 2004 / Received in final form 20 July 2004
Published online 30 September 2004 –

Abstract. The magnetic properties of the polymerized phase of RbC_{60} have been investigated by static magnetization measurements. The magnetic susceptibility comprises a temperature dependent part that decreases rapidly below 50 K, where the metal-insulator transition and the subsequent antiferromagnetic ordering are expected according to electron spin resonance results. The temperature variation of this contribution resembles that of quasi-one-dimensional gapped systems and shows substantial field dependence suggesting a disordered antiferromagnetic phase.

PACS. 61.48.+c Fullerenes and fullerene-related materials – 75.50.Ee Antiferromagnetics – 71.30.+h Metal-insulator transitions and other electronic transitions

1 Introduction

The stable polymeric phase of the alkali-doped fullerides AC_{60} (A = K, Rb, Cs) forming upon slow cooling from the high-temperature fcc phase has stimulated intensive research due to the subtle interplay between structural, magnetic and electronic properties [1,2]. A metal-insulator transition was ascertained below 50 K by electron spin resonance (ESR) and conductivity experiments on both RbC_{60} and CsC_{60} polymers [2,3]. Despite extensive studies, the origin of this transition remains controversial as both a spin-density wave (SDW) instability characteristic of quasi-one-dimensional (1D) metals [2–4] and antiferromagnetic (AFM) ordering of a three-dimensional (3D) system [5,6] have been proposed. In particular, the presence of antiferromagnetic resonance suggestive of the SDW ground state was revealed by high-field ESR [4], while persistent 1D spin fluctuations up to room temperature along with the low-T AFM ordering was inferred from nuclear magnetic resonance (NMR) [7]. However, subsequent ESR studies showed that although antiferromagnetic resonance can not be excluded below 25−30 K, a spin-glass-like behavior may be also implicated [8]. Similarly, earlier muon-spin relaxation (μSR) studies failed to identify long-range magnetic order as in regular antiferromagnets or SDW systems but rather a transition to a disordered magnetic state [9–11]. Analysis of the ESR lineshapes of RbC_{60} has also implied that structural disorder and localized paramagnetic defects could result in the spread of the transition temperatures and the development of short-range order [12,13].

Density functional calculations have predicted that the electronic properties retain a strongly 3D-character due to the rehybridization of carbon orbitals and the large molecular coordination in the transverse direction to the polymer chains [5], further corroborated by theoretical studies of the chain-orientation dependence of the RbC_{60} electronic structure [14]. A pressure dependent phase diagram has been accordingly constructed for RbC_{60} exploiting resistivity [15] and ESR results, indicating a 3D Mott-Hubbard system with AFM order at low temperatures [6]. Essentially isotropic electronic properties have been also derived from the analysis of both the ^{13}C NMR spectra in CsC_{60} showing that the spin density is concentrated near the equator of the C_{60} molecules and thus favors substantial interchain coupling [16], as well as ESR studies of the reduced g-anisotropy [17] and the scattering rate of RbC_{60} [18]. Static magnetic susceptibility measurements that have elucidated the SDW ground state of quasi-1D organic salts like $(TMTSF)_2PF_6$ [19], have been only recently reported for the RbC_{60} polymer revealing a reduction of the susceptibility below 50 K [20]. This behavior has been analyzed within the SDW approach, relying on the quasi-1D electronic properties of RbC_{60} predicted for a narrow range of chain orientation angles [14], which are, however, incompatible with the value of 46−47° determined by thorough structural studies [21,22].

In this work, we have performed a systematic study of the field and temperature dependence of the static magnetization for the polymeric phase of RbC_{60} complemented by ESR measurements. A temperature-dependent contribution resembling that of quasi-1D gapped systems is deduced that decreases rapidly below 50 K, where

[a] e-mail: sglenis@cc.uoa.gr

AFM ordering is expected. Appreciable field dependence is observed suggesting an inhomogeneous magnetic ground state of RbC_{60}.

2 Experimental

RbC_{60} powder samples were prepared by the solid state reaction of stoichiometric amounts of C_{60} with Rb in sealed, evacuated quartz tubes, properly polymerized by slow cooling from high temperatures. Magnetic measurements were performed using a Quantum Design MPMS SQUID magnetometer in the temperature range of 5−300 K and magnetic fields up to 50 kG. The diamagnetic contribution of the support cell was independently measured and subtracted. To verify the AFM transition for the RbC_{60} polymer sample, ESR measurements were performed on a standard Bruker X-band spectrometer (ν = 9.42 GHz) with 100 kHz field modulation. An Oxford flow cryostat was used for temperature dependent measurements (4−300 K).

3 Results and discussion

Figure 1 shows representative ESR spectra of the RbC_{60} sample as a function of temperature, which can be accurately fitted to a single Lorentzian lineshape over a broad temperature range. However, deviations from the single Lorentz fit occur at $8 < T < 30$ K, which can be taken into account by the superposition of a broader Lorentzian line (Fig. 1). Figure 2 summarizes the temperature dependence of the total integral ESR intensity I_{ESR}, which is proportional to the spin susceptibility, normalized to the high temperature value and the resonance linewidth of the dominant narrow ESR line. A rapid drop of I_{ESR} below 50 K signals the opening of a gap in the spin excitation spectrum, followed by a shallow minimum at $T \approx 15$ K, below which a slight increase is detected. Despite its low amplitude, the intensity of the broad ESR component is not negligible amounting to about 10 to 30% of the total I_{ESR}, depending on T, and follows qualitatively the same temperature variation, though with a clear minimum at 15 K. The ESR linewidth broadens rapidly below 40 K, suggestive of the slowing down of spin fluctuations and the growth of internal fields as AFM ordering is approached. At $T > 50$ K, the linewidth increases sublinearly with temperature, complying with the conduction electron spin relaxation caused by spin-orbit scattering on phonons and defects [18]. Overall, these results are in good agreement with previous ESR studies [2,4,6,8,12,13], validating subsequent dc magnetization measurements on the same sample.

Figure 3 shows the field and temperature dependence of the static magnetization $M(H,T)$. A rapid increase of the isothermal magnetization $M(H)_T$ curves is observed at low fields [Fig. 3a] as well as large differences between the magnitude of M/H that decreases with increasing magnetic field [Fig. 3b]. Both these features indicate the

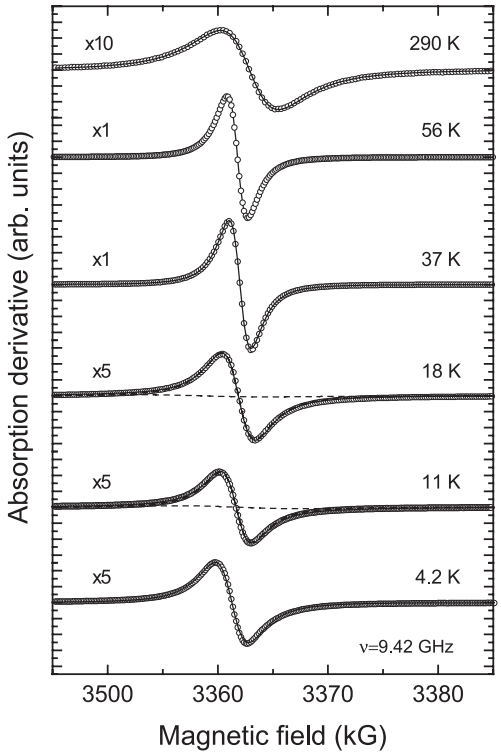

Fig. 1. Temperature dependence of the X-band ESR spectra for RbC_{60}. Lines correspond to the best fit Lorentz lineshapes for the total spectrum (solid line) and its two components (dashed lines).

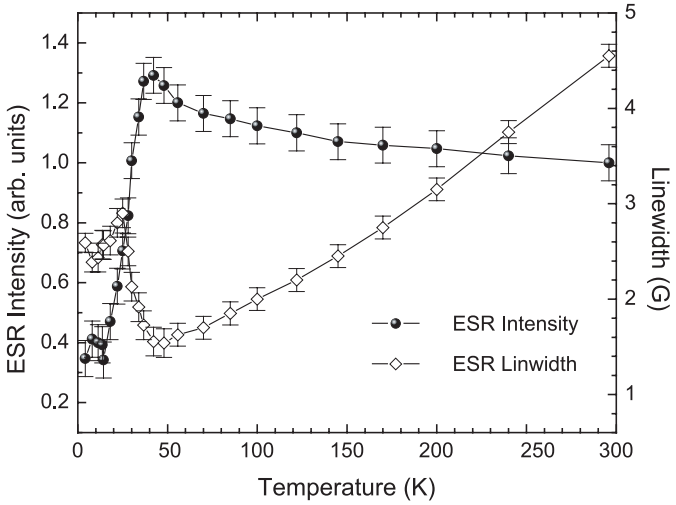

Fig. 2. Temperature dependence of the total ESR intensity and the resonance linewidth for RbC_{60} at the X-band.

presence of ferromagnetic impurities, in agreement with previous results on RbC_{60} [20]. To obtain an estimate of the ferromagnetic contribution, the magnetization curves have been analyzed using $M(H,T) = M_{FM} + \Delta M = M_{FM}L(\mu H/kT) + M_0 B_{1/2}(x)$, where $L(\mu H/kT)$ is the Langevin function with μ the average moment per ferromagnetic particle and M_{FM} the corresponding saturation magnetization, while $B_{1/2}(x)$ is the Brillouin function

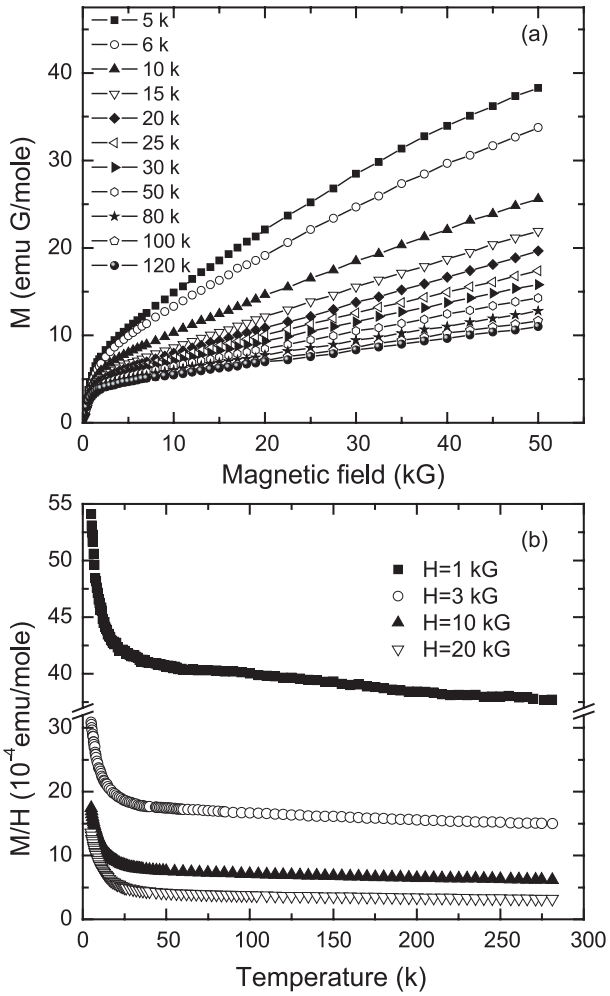

Fig. 3. (a) Field dependence of the static magnetization $M(H)$ at various temperatures, and (b) temperature dependence of M/H at different magnetic fields for RbC_{60}.

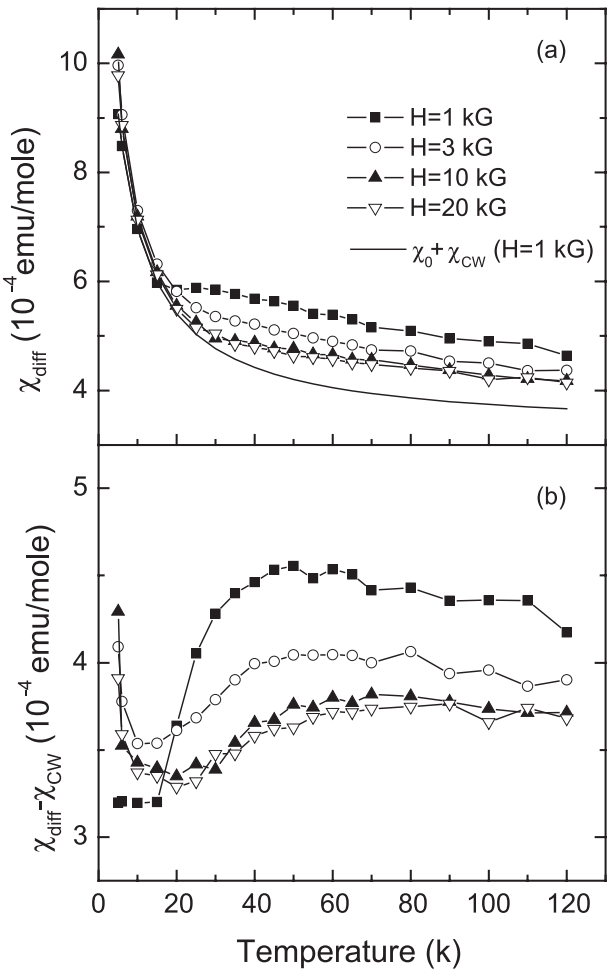

Fig. 4. (a) Temperature dependence of the differential static susceptibility χ_{diff} at different magnetic fields. The solid line represents the best fit of the low-T susceptibility to $\chi_0 + \chi_{CW}$ at $H = 1$ kG. (b) Temperature dependence of the difference $\Delta\chi = \chi_{diff} - \chi_{CW}$ ($H = 1$ kG) at the same magnetic fields.

with $x = gS\mu_B H/kT$ and $M_0 = NgS\mu_B$ for paramagnetic $S = 1/2$ spins with $g = 2.0$. Prior to this analysis all raw data were corrected for a core diamagnetic susceptibility of -2.74×10^{-4} emu/mole [20,23]. An effective description of the $M(H)_T$ data could be thus obtained for different values of μ at various temperatures and an increasing saturation magnetization M_{FM} at low temperatures ($T \leq 10$ K). The resulting magnetization curves $\Delta M = M - M_{FM}$ do not scale with a single paramagnetic $S = 1/2$ Brillouin function at different temperatures. Instead, if paramagnetic spins with $S = 1/2$ are assumed, a continuous reduction of the spin concentration N is observed as temperature decreases, indicative of antiferromagnetic correlations.

Subsequently, the temperature dependence of the differential static susceptibility $\chi_{diff}(T) = [\partial(\Delta M)/\partial H]_T$ was derived from the $\Delta M(H)$ data, as shown in Figure 4a. The susceptibility is thus found to vary slowly down to $T \approx 20$ K, whereas a paramagnetic-like upturn turns out to be dominant at lower temperatures. No clear anomaly of $\chi_{diff}(T)$ could be resolved in the temperature range of 25−35 K, where the AFM transition is expected, except for a small but distinct field dependence at magnetic fields $H < 10$ kG. This behavior is in contrast to the spin susceptibility χ_s determined from the X-band ESR intensity. In the latter case, 3D AFM fluctuations above $T_N \simeq 35$ K followed by the presence of antiferromagnetic resonance at lower temperatures have been proposed to broaden the ESR line beyond detection [4]. On the other hand, the absolute value of χ_{diff} at $T > 50$ K approaches the corresponding spin susceptibility χ_s. In particular, χ_{diff} is about 70% of $\chi_s \simeq 7 \times 10^{-4}$ emu/mole [2]. This discrepancy may be due to overestimates of the diamagnetic and/or ferromagnetic corrections. In either case, the increase of χ_{diff} at $T < 20$ K, should be detectable by ESR, unless excessive broadening or shift of the underlying resonance occurs. This would indicate that the low-T rise of χ_{diff} is not entirely due to paramagnetic impurities but may also reflect intrinsic contributions such as those observed in the AFM ground state of SDW organic conductors, perpendicular to the easy magnetization

axis [19,24]. In order to analyze further the temperature variation of χ_{diff}, we may assume that the low-T upturn can be effectively described in terms of a temperature independent term χ_0 and a Curie-Weiss term $\chi_{CW} = C/(T - \Theta)$. These two contributions have been determined by fitting the $\chi_{diff}(T)$ data for $H = 1$ kG at $T \leq 15$ K, yielding $\chi_0 = 0.00032(3)$ emu/mole, a Curie constant of $C = 0.0051(3)$ emu K/mole and a Curie-Weiss temperature $\Theta = -3(1)$ K. Subtracting the latter component from $\chi_{diff}(T)$ yields a nearly constant susceptibility $\Delta\chi = \chi_{diff} - \chi_{CW}$ at higher temperatures that decreases rapidly below $T \simeq 50$ K, as shown in Figure 4b. This behavior is in good agreement with the temperature variation of I_{ESR}, while the magnitude of $\Delta\chi$ at $T = 100$ K is approximately 65% of the spin susceptibility $\chi_s(100\,\text{K}) \simeq 7{\times}10^{-4}$ emu/mole [2]. Furthermore, subtraction of χ_{CW} from $\chi_{diff}(T)$ at higher fields reveals a gradual reduction of the high-T susceptibility and a smoother temperature variation [Fig. 4b].

To explore the field and temperature dependence of the static susceptibility the $M(T)$ data, where the resolution of the experimental points is higher, have been accordingly analyzed. Figure 5a shows the temperature dependence of the static susceptibility derived from the ratio $\Delta M/H = (M - M_{FM})/H$ for different magnetic fields. In this case, the temperature dependence of M_{FM} has been determined from the corresponding $M(H)_T$ curves up to 120 K and then extrapolated up to high temperatures. The resulting plots of $\Delta M/H$ vs. T are similar to $\chi_{diff}(T)$ up to 120 K, including the paramagnetic-like upturn at low temperatures. However, a broad local maximum is observed for magnetic fields of 1 and 3 kG at $T \approx 100$ K, which is suppressed at higher fields, and a small increase of the low-T susceptibility below 20 K as the magnetic field increases, most clearly seen in the inset of Figure 5a. Performing the same decomposition as for $\chi_{diff}(T)$, namely fit of the low-T susceptibility at $H = 1$ kG to a Curie-Weiss law, results in the best fit values of $\chi_0 = 0.00031(2)$ emu/mole, $C = 0.0053(2)$ emu K/mole for the Curie constant and $\Theta = -2.0(5)$ K for the Curie-Weiss temperature, similar to those obtained from the analysis of the differential susceptibility. Subtracting the χ_{CW} component from $\Delta M/H$ reveals the broad maximum at $T \approx 75$ K, most prominent for the smaller magnetic fields, followed by a rapid decrease of the susceptibility below 50 K, as shown in Figure 5b. At higher magnetic fields, a gradual smearing of the rounded maximum of $\Delta\chi$ is observed and a smoother temperature variation leading eventually to a crossover of the susceptibility at $T \approx 20$ K for different applied fields. This behavior generally agrees with the temperature dependence of the differential susceptibility $\Delta\chi$ up to 120 K, yet the field dependence of the static susceptibility appears to persist even at high temperatures resembling the behavior of spin-glass like systems. To this aim, the temperature dependence of the zero-field cooled (ZFC) and field cooled (FC) magnetization was subsequently measured at different magnetic fields. A small splitting of the corresponding ZFC and FC M/H curves was indeed observed below approximately 50 K only for

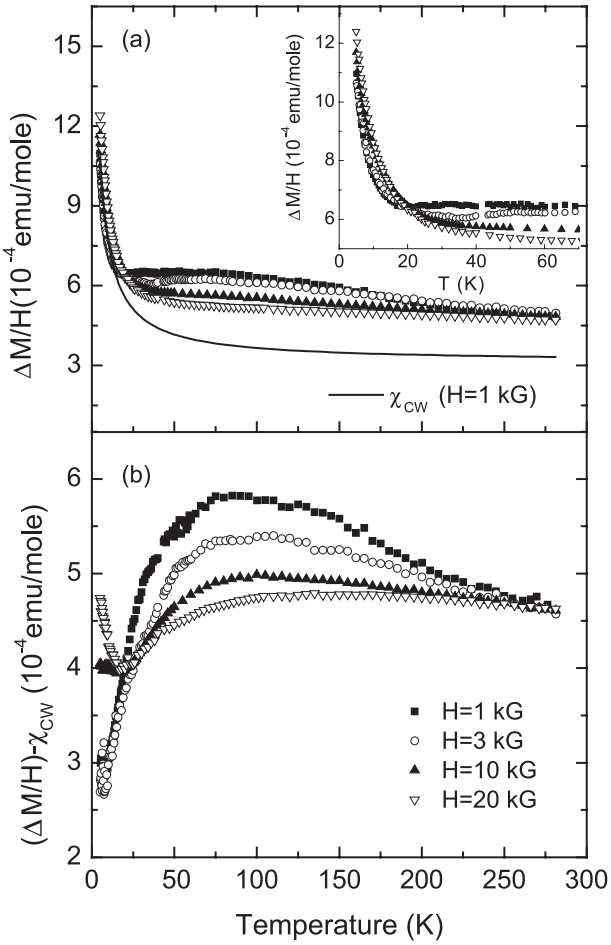

Fig. 5. (a) Temperature dependence of $\Delta M/H = (M - M_{FM})/H$ for different magnetic fields. The solid line represents the best fit of $\Delta M/H$ to $\chi_0 + \chi_{CW}$ at $H = 1$ kG and $T \leq 15$ K. The inset shows in more detail the variation of $\Delta M/H$ below 100 K. (b) Temperature dependence of $(\Delta M/H) - \chi_{CW}$ ($H = 1$ kG) for the same applied fields.

$H = 10$ kG, whereas no appreciable irreversibility was traced for smaller fields, as shown in Figure 6. Subtraction of the low-temperature Curie-Weiss part from both the ZFC and FC magnetization data, showed a slight but clear hysteresis unlike that of canonical spin-glasses, where pronounced irreversibility between the ZFC and FC magnetization is frequently observed at low magnetic fields. Moreover, relaxation measurements of the remanent magnetization at 6 K after turning off the magnetic field applied typically for 5 minutes did not show any appreciable time decay as would be expected for a spin-glass system. In that case, a disordered AFM ground state may be invoked that would comply with the random static order suggested by μSR experiments [9–11].

A disordered AFM phase for RbC_{60} has been previously inferred from the analysis of the ESR lineshapes showing multiple active sites [12,13], similar to the present ESR results, as well as the increased contribution of impurity scattering in the ESR linewidth [18]. This was rationalized by the presence of structural disorder mainly

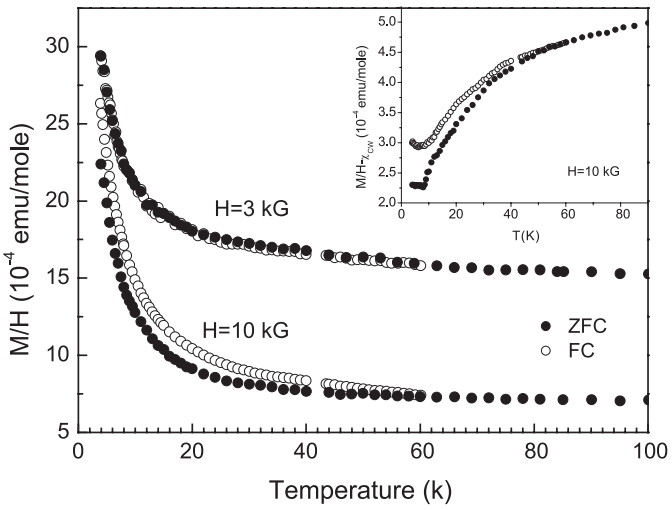

Fig. 6. Temperature dependence of the ZFC and FC magnetization at magnetic fields of 3 and 10 kG. The inset shows the resulting $(M/H) - \chi_{CW}$ curves at $H = 10$ kG.

due to the finite polymer chain length and the possible presence of paramagnetic defects. On the other hand, pressure-dependent NMR studies have shown that CsC_{60}, considered to exhibit similar electronic properties with RbC_{60}, undergoes a transition to a non-magnetic state at $T_s = 13.8$ K coexisting with magnetic order [25,26]. The structural origin of this transition has been clearly evinced by high-resolution synchrotron X-ray diffraction showing a spontaneous lattice contraction below 14 K and thus significant magnetoelastic coupling [27]. A dynamically inhomogeneous state has been then suggested involving both localized spins and mobile polarons that compete with 3D AFM order imposed by the transverse coupling between the polymer chains. It is worth noting that the observed $\chi(T)$ variation can be well described with the thermally activated dependence of the static susceptibility [20], inherently occurring on the low-T approximation for both gapped 1D AFM Heisenberg chains [28] and 1D-conductors [29] due to the quadratic dependence of the dispersion relation near the band minimum. The temperature variation of χ preserving the generic features of low-dimensional systems might then support an electronically driven inhomogeneity due to disordered AFM chains. In this respect, the field dependence of the susceptibility may be related to either chemical inhomogeneity anticipated from structural disorder or even electronic phase separation caused by the coexistence of localized spins and mobile polarons.

4 Conclusions

In conclusion, static magnetization measurements on the RbC_{60} polymerized phase show that no distinct anomaly corresponding to the antiferromagnetic transition identified by ESR is observed. The bulk magnetic susceptibility exhibits a relatively slow temperature variation up to $T \simeq 20$ K and a small paramagnetic-like upturn at lower temperatures. Subtraction of the latter contribution reveals a temperature and field dependent part rapidly decreasing below 50 K, where AFM ordering is expected to set out according to the ESR data. The temperature dependence of the latter contribution resembles closely that of quasi-1D gapped systems. The observed field dependence sustained from high temperatures is attributed to a disordered AFM phase, further supported by a small irreversible behavior of the ZFC and FC magnetization at a relatively high magnetic field of 10 kG.

We would like to thank Professor K. Prassides for kindly providing the RbC_{60} polymer samples.

References

1. P.W. Stephens, G. Bortel, G. Faigel, M. Tegze, A. Jánossy, S. Pekker, G. Oszlányi, L. Forró, Nature (London) **370**, 636 (1994)
2. O. Chauvet, G. Oszlányi, L. Forró, P.W. Stephens, M. Tegze, G. Faigel, A. Jánossy, Phys. Rev. Lett. **72**, 2721 (1994)
3. F. Bommeli, L. Degiorgi, P. Wachter, O. Legeza, A. Jánossy, G. Oszlányi, O. Chauvet, L. Forró, Phys. Rev. B **51**, 14794 (1995)
4. A. Jánossy, N. Nemes, T. Féher, G. Oszlányi, G. Baumgartner, L. Forró, Phys. Rev. Lett. **79**, 2718 (1997)
5. S.C. Erwin, G.V. Krishna, E.J. Mele, Phys. Rev. B **51**, 7345 (1995)
6. H. Sakamoto, S. Kobayashi, K. Mizoguchi, M. Kosaka, K. Tanigaki, Phys. Rev. B **62**, R7691 (2000)
7. V. Brouet, H. Alloul, Y. Yoshinari, L. Forró, Phys. Rev. Lett. **76**, 3638 (1996)
8. M. Bennati, R.G. Griffin, S. Knorr, A. Grupp, M. Mehring, Phys. Rev. B **58**, 15603 (1998)
9. Y.J. Uemura, K. Kojima, G.M. Luke, W.D. Wu, G. Oszlányi, O. Chauvet, L. Forró, Phys. Rev. B **52**, R6991 (1995)
10. W.A. MacFarlane, R.F. Kiefl, S. Dunsiger, J.E. Sonier, J.E. Fischer, Phys. Rev. B **52**, R6995 (1995)
11. L. Cristofolini, A. Lappas, K. Vavekis, K. Prassides, R. DeRenzi, M. Ricco, A. Schenk, A. Amato, F.N. Gygax, M. Kosaka, K. Tanigaki, J. Phys.: Condens. Matter **7**, L567 (1995)
12. V.A. Atsarkin, V.V. Demidov, G.A. Vasneva, Phys. Rev. B **56**, 9448 (1997)
13. K. Mizoguchi, A. Sasano, H. Sakamoto, M. Kosaka, K. Tanigaki, T. Tanaka, T. Atake, Synth. Metals **103**, 2395 (1999)
14. T. Saito, Y. Akita, H. Kobayshi, K. Tanaka, Synth. Metals **113**, 45 (2000)
15. K. Khazeni, V.H. Crespi, J. Hone, A. Zettl, M.L. Cohen, Phys. Rev. B **56**, 6627 (1997)
16. T.M. de Swiet, J.L. Yarger, T. Wagberg, J. Hone, B.J. Gross, M. Tomaselli, J.J. Titman, A. Zettl, M. Mehring, Phys. Rev. Lett. **84**, 717 (2000)
17. J. Rahmer, A. Grupp, M. Mehring, J. Hone, A. Zettl, Phys. Rev. B **63**, 081108 (2001)
18. J. Rahmer, A. Grupp, M. Mehring, Phys. Rev. B **64**, 235405 (2001)

19. K. Mortensen, Y. Tomkiewicz, T.D. Schultz, E.M. Engler, Phys. Rev. Lett. **46**, 1234 (1981); K. Mortensen, Y. Tomkiewicz, K. Bechgaard, Phys. Rev. B **25**, 3319 (1982)
20. T. Saito, Y. Akita, K. Tanaka, Phys. Rev. B **61**, 16091 (2000)
21. P. Launois, R. Moret, J. Hone, A. Zettl, Phys. Rev. Lett. **81**, 4420 (1998)
22. A. Huq, P.W. Stephens, G.M. Bendele, R.M. Ibberson, Chem. Phys. Lett. **347**, 13 (2001)
23. A.P. Ramirez, R.C. Haddon, O. Zhou, R.M. Fleming, J. Zhang, S.M. McClure, R.E. Smalley, Science **265**, 84 (1994)
24. J.C. Scott, H.J. Pedersen, K. Bechgaard, Phys. Rev. Lett. **45**, 2125 (1980)
25. B. Simovič, D. Jérome, F. Rachdi, G. Baumgartner, L. Forró, Phys. Rev. Lett. **82**, 2298 (1999)
26. B. Simovič, D. Jérome, L. Forró, Phys. Rev. B **63**, 125410 (2001)
27. S. Ruzière, S. Margadonna, K. Prassides, A.N. Fitch, Europhys. Lett. **51**, 314 (2000)
28. D.C. Johnston, R.K. Kremer, M. Troyer, X. Wang, A. Klümper, S.L. Bud'ko, A.F. Panchula, P.C. Canfield, Phys. Rev. B **61**, 9558 (2000)
29. D.C. Johnston, Phys. Rev. Lett. **52**, 2049 (1984)